Global feedback control for pattern-forming systems

L. G. Stanton and A. A. Golovin
Department of Engineering Sciences and Applied Mathematics, Northwestern University, Evanston, Illinois 60208, USA
(Received 6 June 2007; published 20 September 2007)

Global feedback control of pattern formation in a wide class of systems described by the Swift-Hohenberg (SH) equation is investigated theoretically, by means of stability analysis and numerical simulations. Two cases are considered: (i) feedback control of the competition between hexagon and roll patterns described by a supercritical SH equation, and (ii) the use of feedback control to suppress the blowup in a system described by a subcritical SH equation. In case (i), it is shown that feedback control can change the hexagon and roll stability regions in the parameter space as well as cause a transition from up to down hexagons and stabilize a skewed (mixed-mode) hexagonal pattern. In case (ii), it is demonstrated that feedback control can suppress blowup and lead to the formation of spatially localized patterns in the weakly nonlinear regime. The effects of a delayed feedback are also investigated for both cases, and it is shown that delay can induce temporal oscillations as well as blowup.

DOI: 10.1103/PhysRevE.76.036210 PACS number(s): 89.75.Kd

I. INTRODUCTION

Spatiotemporal pattern formation in systems far from equilibrium has been a subject of active research in physics, chemistry, and biology for several decades [1–4]. Recently, the manipulation of pattern-forming processes by applying feedback control has been attracting growing attention [5,6]. It has been shown that feedback control can be successfully used to manipulate Rayleigh-Bénard convection [7–10], Marangoni convection [11–13], convection in binary systems [14], contact line instability in thin liquid films [15,16], shear flows [17–20], excitable media [21–24] and other reaction-diffusion systems [25], catalytic reactions [26–28], patterns in nonlinear optics [29,30], crystal growth [31,32], cardiac dynamics [33], and other systems as well.

A characteristic feature of pattern-forming systems is that they can be divided into several large classes depending on the type of instability, basic symmetries, and conservation laws present in the system. Within each class, the system's nonlinear dynamics near the instability threshold is governed by a generic evolution equation, such that the whole plethora of pattern-forming systems can be described by a few such equations [3,4,39]. Thus, the feedback control of pattern formation in many systems can be studied by using models based on generic nonlinear evolution equations. For example, feedback control of wave dynamics, typical of systems exhibiting oscillatory instabilities, has been studied using the generic complex Ginzburg-Landau equation [34–38]. The possibility of feedback control of chaotic dynamics in systems with translation invariance exhibiting long-wave instability that are described by a generic Kuramoto-Sivashinsky equation (such as flame fronts [40], solidification fronts [41–43], liquid film flow [44,45], and chemical oscillations [46]) was studied in [47–49].

A large class of spatially isotropic systems that exhibit the formation of stationary roll (stripe) or hexagonal patterns resulting from a monotonic instability of a spatially homogeneous state is described by a Swift-Hohenberg (SH) equation [3,50,51] for the "order parameter" $\phi(\mathbf{x},t)$ that can be written in a rescaled form as

$$\frac{\partial \phi}{\partial t} = \gamma\phi - (1+\nabla^2)^2\phi + \alpha\phi^2 - \beta\phi^3. \tag{1}$$

Equation (1) is used to model the nonlinear dynamics of Rayleigh-Bénard and Marangoni convection, diblock copolymerization, and many other systems [3,50,52], and has been extensively studied. The quadratic term is present to include systems with broken reflection symmetry of the order parameter. In fluid convection, this corresponds to thermocapillary effects or non-Boussinesq fluids [52]. The parameter γ characterizes the linear growth rate and is proportional to the distance of the bifurcation parameter from the instability threshold, and $\beta=\pm 1$. The case $\beta=1$ corresponds to a supercritical instability in which Eq. (1) describes relaxational dynamics leading to the formation of roll or hexagonal patterns. The case $\beta=-1$ corresponds to a subcritical instability in which Eq. (1) leads to a blowup in finite time and does not describe pattern formation dynamics. In this case, one can argue that higher-order nonlinearities start playing a role, and one should add a quintic nonlinear term to Eq. (1) in order to describe the nonlinear dynamics. The quintic SH equation, describing pattern formation in systems exhibiting a subcritical instability, has also been extensively studied [53,54].

Feedback control of systems described by a supercritical SH equation in one dimension (1D) was first considered in [55]. It was shown that applying *localized* feedback at a few spatial locations can stabilize both uniform and pattern states. In the present paper, we investigate the possibility of applying a *global* feedback control to a pattern-forming system whose dynamics is described by a Swift-Hohenberg equation in 2D. By global feedback control, we mean that, based on the measurements of some global characteristic of the system, we vary some parameter that determines the system behavior in the whole domain. Such types of control might be easier to implement experimentally. We shall focus on the following two questions: (i) Can global feedback control change the competition between roll and hexagonal patterns? (ii) Can global feedback control suppress the blowup in a subcritical SH equation and keep the system dynamics in a weakly nonlinear regime? Since both the roll-hexagon

competition and the subcritical pattern blowup are associated with growing amplitude of the pattern, we choose a global feedback control based on measuring the maximum of the pattern amplitude over the domain. Thus, we consider the following two cases: (i) feedback control of roll-hexagon competition in a supercritical SH equation ($\beta=1$); (ii) feedback control of blowup in a subcritical SH equation ($\beta=-1$). In case (i), since the presence of hexagonal patterns is due to the quadratic term in Eq. (1), we choose to apply feedback control to the parameter α characterizing the reflection symmetry breaking and consider

$$\alpha[\phi] = \alpha_0 + p \max_x\{|\phi(t-\tau)|\}. \tag{2}$$

This can be done experimentally, say, by applying an external field tuned according to the measurements of $\max_x|\phi|$. The delay τ has been included to allow for any experimental elapse in time between the sensor measurements and the adjustments of actuators in the feedback loop. In many cases, however, this time delay is small in comparison to the temporal evolution of the system and can be neglected. In case (ii), we consider controlling the supercriticality γ and set

$$\gamma[\phi] = \gamma_0 - p \max_x\{|\phi(t-\tau)|\}, \quad p>0. \tag{3}$$

This can be implemented in a laboratory by changing the parameter governing the instability driving force (for instance, the temperature difference across a liquid layer in the case of convection), and this type of global feedback was also considered in [32,38].

The paper is structured as follows. In Sec. II, we consider feedback control without delay of the competition between rolls and hexagons. In Sec. III, we investigate the possibility of suppressing the blowup in a system described by a subcritical SH equation, via feedback control without delay in order to keep the system dynamics in a weakly nonlinear regime. In Sec. IV, we investigate the effects of delay in the feedback loop. Conclusions are presented in Sec. V.

II. FEEDBACK CONTROL OF HEXAGON-ROLL COMPETITION

Here we consider the following model describing the SH dynamics in the presence of feedback control of the symmetry-breaking quadratic term with a negligible delay ($\tau=0$):

$$\frac{\partial\phi}{\partial t} = \gamma\phi - (1+\nabla^2)^2\phi + \alpha[\phi]\phi^2 - \phi^3, \tag{4a}$$

$$\alpha[\phi] = \alpha_0 + p \max_x\{|\phi|\}. \tag{4b}$$

Since Eqs. (4a) and (4b) are invariant with respect to the transformation $\alpha_0\to-\alpha_0$, $\phi\to-\phi$, $p\to-p$, we will restrict our attention to $\alpha_0\geq 0$.

Equations (4a) and (4b) have the trivial solution $\phi\equiv 0$. Small perturbations of this solution, $\tilde{\phi}\sim e^{\sigma t+i\mathbf{k}\cdot\mathbf{x}}$, are characterized by the dispersion relation $\sigma=\gamma-(1-k^2)^2$, where $k=|\mathbf{k}|$. The trivial state is unstable for $\gamma>0$, and the instability onset corresponds to $k=k_c\equiv 1$.

Consider the system (4a) and (4b) near the instability threshold: $\gamma=O(\epsilon^2)$, $0<\epsilon\ll 1$. We introduce the slow time $T=\epsilon^2 t$, assume $p=O(1)$, $\alpha_0=O(\epsilon)$, and expand $\phi=\epsilon\phi_1+\epsilon^2\phi_2+\epsilon^3\phi_3+\cdots$, where $\phi_1=A_1(T)e^{i\mathbf{k}_1\cdot\mathbf{x}}+A_2(T)e^{i\mathbf{k}_2\cdot\mathbf{x}}+A_3(T)e^{i\mathbf{k}_3\cdot\mathbf{x}}+$c.c. (with $\mathbf{k}_1+\mathbf{k}_2+\mathbf{k}_3=0$, $|\mathbf{k}_{1,2,3}|=1$). Since the competition between rolls and hexagons is governed by amplitude rather than modulational instabilities, we neglect here spatial modulations of the complex amplitudes $A_{1,2,3}(T)$. The effect of spatial modulations could be taken into account within the framework of more general models [56–59]; however, as seen below, the predictions based on the Landau-type equations are verified by numerical simulations of Eqs. (4a) and (4b). By means of a standard multiple-scale analysis (see [4], Chap. 4.4), one obtains the following system of amplitude equations for the complex amplitudes $A_{1,2,3}(T)$:

$$\dot{A}_1 = \gamma A_1 - (3|A_1|^2+6|A_2|^2+6|A_3|^2)A_1 + 2A_2^*A_3^*\left(\alpha_0 + 2p\sum_{n=1}^{3}|A_n|\right), \tag{5}$$

where the two other equations are obtained via cyclic permutations of the indices, and $(\cdot)$ denotes differentiation with respect to T.

A. Stability of rolls

We first rewrite our complex amplitudes in polar form as $A_n=R_n\exp(i\theta_n)$ and define $\Theta=\theta_1+\theta_2+\theta_3$. To examine the stability of a roll pattern, consider one of the three stationary solutions of the system (5): $R_1=R=\sqrt{\gamma/3}$, $R_2=R_3=0$. For infinitesimal perturbations $\tilde{R}_n\sim e^{\sigma T}$ of this solution, we see that one mode is always damped, and, for the two remaining modes, we obtain a quadratic dispersion relation that has the roots $\sigma=-\gamma\pm[2\alpha_0\sqrt{\gamma/3}+(4/3)p\gamma]$. Thus, the rolls are stable for

$$\left|\frac{2\alpha_0}{\sqrt{3\gamma}}+\frac{4p}{3}\right|<1. \tag{6}$$

One can see that, in the absence of control ($p=0$), the condition (6) reduces to the usual condition for roll stability, $\gamma>4\alpha_0^2/3$.

B. Stability of hexagons

Now consider the stationary solution of the system (5) corresponding to a hexagonal pattern, $R_1=R_2=R_3=R$, where

$$R=\frac{\alpha_0 q_h \pm \sqrt{\alpha_0^2+(15-12q_hp)\gamma}}{15-12q_hp}, \quad q_h=\mathrm{sgn}(\alpha_0+6pR). \tag{7}$$

The solution (7) clearly exists only for $\alpha_0^2+(15-12q_hp)\gamma>0$. Since $\alpha_0>0$, then $q_h=1$ for $p>0$. If $p<0$, $q_h=1$ for $0<R<\alpha_0/(6|p|)$, and $q_h=-1$ for $R>\alpha_0/(6|p|)$. This flip in sign results in a change in stability of the attracting manifold for Θ. Hence, for $p<0$, one observes a transition from up hexagons (the order parameter has a maximum in the center of the hexagonal cell) to down hexagons (the order param-

eter has a minimum in the center), when the pattern amplitude exceeds the critical value $R_c=\alpha_0/(6|p|)$.

For infinitesimal perturbations $\tilde{R}_n \sim e^{\sigma T}$ of the solution (7), one obtains the following dispersion relation: $[\sigma-(a+2b)][\sigma-(a-b)]^2=0$, where $a=-2\alpha_0 q_h R-(8q_h p+6)R^2$ and $b=2\alpha_0 q_h R+(16q_h p-12)R^2$. This leads to the two stability conditions

$$0 > a+2b = \mp 2R\sqrt{\alpha_0^2+(15-12q_h p)\gamma},$$

$$0 > a-b = 2\gamma - 24R^2. \tag{8}$$

From (8), we obtain that the lower branch of the steady-state solution (7) is always unstable, and the stability condition for the upper branch is

$$1 < \left| \frac{4\alpha_0}{\sqrt{3\gamma}} + 4p \right|. \tag{9}$$

In the absence of feedback ($p=0$), the condition (9) reduces to the usual condition for hexagon stability, $\gamma < 16\alpha_0^2/3$.

C. Stability of mixed modes

The system (5) has a third stationary solution in the form $R_1=R$, $R_2=R_3=mR(m\geq 0)$, where

$$R = \frac{(6q_m-8p)\alpha_0 \pm \frac{8}{3}p\sqrt{\left(\frac{112}{3}p^2-24q_m p+9\right)\gamma-12\alpha_0^2}}{\frac{112}{3}p^2-24q_m p+9},$$

$$mR = \frac{1}{3}\sqrt{\gamma-3R^2}, \quad q_m = \mathrm{sgn}[\alpha_0+(2+4m)pR]. \tag{10}$$

It describes the so-called *mixed mode* or *skewed hexagons* and separates the basins of attraction of rolls and hexagons. In the absence of feedback, this mode corresponds to $R_1=2\alpha_0/3$, $R_2=R_3=\frac{1}{3}\sqrt{\gamma-4\alpha_0^2/3}$, and it is always unstable (see [4], Chap. 4.4). As we show below, however, feedback control can stabilize this solution.

Indeed, for infinitesimal perturbations $\tilde{R}_n \sim e^{\sigma T}$ of the solution (10), one obtains the following dispersion relation:

$$[\sigma-(d-e)][\sigma^2-(a+d+e)\sigma+a(d+e)-2bc]=0, \tag{11}$$

where

$$a=[4q_m pm^2-(6+3m^2)]R^2, \quad b=(4q_m pm^2-9m)R^2,$$

$$c=(4q_m pm-9m)R^2, \quad d=[4q_m pm-(3+6m^2)]R^2,$$

$$e=[4q_m pm+(3-12m^2)]R^2.$$

The root $\sigma=d-e=6R^2(m^2-1)$ is negative for $m<1$ and positive otherwise. It means that the mixed mode with $R_1<R_2=R_3$ is always unstable. The remaining quadratic polynomial has roots with negative real parts for $m\in(0,1)$ as long as $(12m-8)p>9m$, and $p<0$. In terms of γ, this stability condition becomes

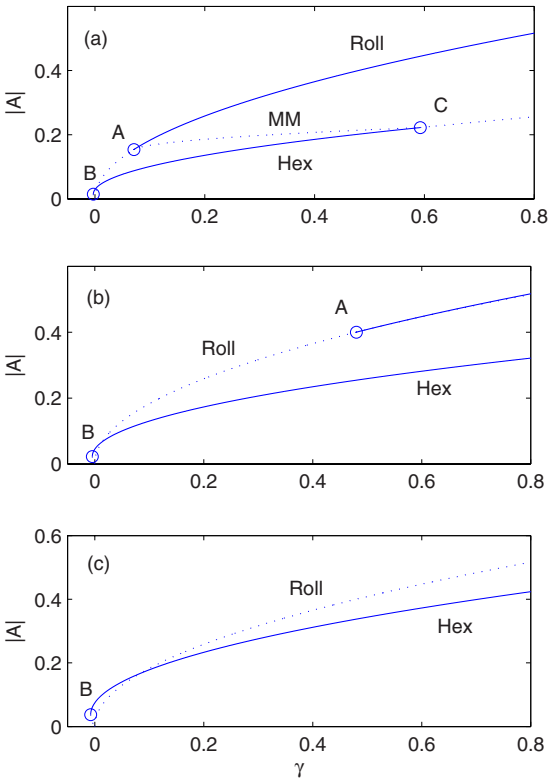

FIG. 1. (Color online) Bifurcation diagrams for $p>0$, $\alpha_0=0.2$. $p=$ (a) 0.1, (b) 0.5, and (c) 0.8. The unstable mixed-mode branch (MM) connects A and C and separates the two basins of attraction.

$$\frac{12\alpha_0^2}{\frac{112}{3}p^2-24p+9} < \gamma < \frac{12\alpha_0^2}{(3-4p)^2} \quad \text{with } p<0. \tag{12}$$

Note that this condition restricts the range of the ratio m to the interval $[0,\frac{2}{3})$, where the neutral stability curve will approach the value $m=\frac{2}{3}$ as $p\to-\infty$.

D. Bifurcation diagrams

The above analysis allows us to plot bifurcation diagrams that show the three types of stationary solution of the system (5) and their stability. Stable branches are represented by solid lines, while unstable branches are represented by dotted lines. The following common notations for the key points on the diagrams are used:

$$A:\gamma=\frac{12\alpha_0^2}{(4p-3)^2}, \quad B:\gamma=\frac{-\alpha_0^2}{15-12p},$$

$$C:\gamma=\frac{48\alpha_0^2}{(12p-3)^2}, \quad D:\gamma=\frac{12\alpha_0^2}{\left(\frac{112}{3}p^2-24p+9\right)},$$

$$E:\gamma=\frac{5\alpha_0^2}{12p^2}, \quad F:\gamma=\frac{48\alpha_0^2}{(12p+3)^2}, \quad G:\gamma=\frac{12\alpha_0^2}{(4p+3)^2},$$

$H:\gamma=-\alpha_0^2/(12p+15)$. For $p>0$, the bifurcation diagrams are shown in Fig. 1. One can see that, with increase of p, the

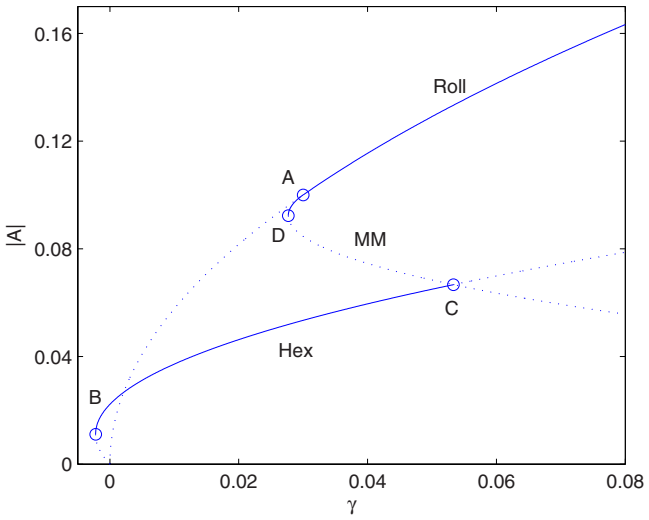

FIG. 2. (Color online) Bifurcation diagram for $p=-0.24$, $\alpha_0=0.2$. A stable branch for the mixed-mode pattern (MM) corresponds to line DA.

stability domains shift to larger values of γ. For $0 \leq p < 1/4$, there is a finite region of bistability between hexagons and rolls. For $p \geq 1/4$, hexagons become unconditionally stable (point C moves to infinity). For $p \geq 3/4$, roll structures become unconditionally unstable (point A moves to infinity). Once $p \geq 5/4$, the strength of the quadratic nonlinearity overpowers the saturation of the cubic term, and the solutions of (4a) and (4b) blow up in finite time.

The dynamics for $p<0$ is far richer. Typical bifurcation diagrams are shown in Figs. 2–6. In this case, the most interesting effect of feedback control is probably that it can stabilize the mixed-mode pattern, which is initially generated by a saddle-node bifurcation and is terminated at the roll solution branch. A typical bifurcation diagram for $-1/4 \leq p < 0$ is shown in Fig. 2. The stable branch of the mixed-mode solution corresponds to line DA.

For $-3/4 \leq p < -1/4$, a finite interval of γ exists in which the hexagonal pattern is unstable. In this interval, either roll

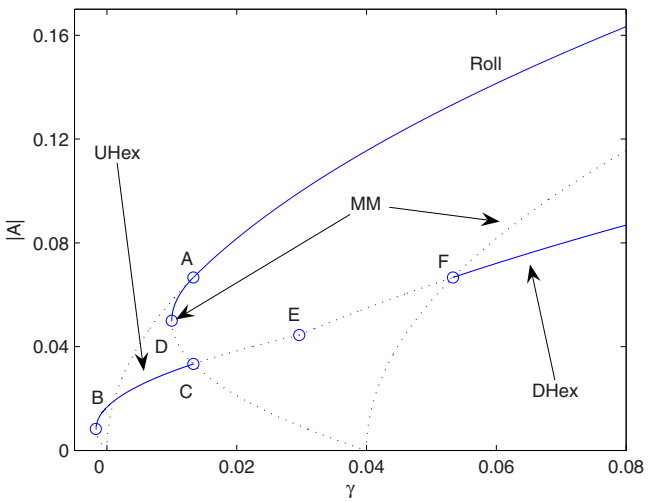

FIG. 3. (Color online) Bifurcation diagram for $p=-0.74$, $\alpha_0=0.2$.

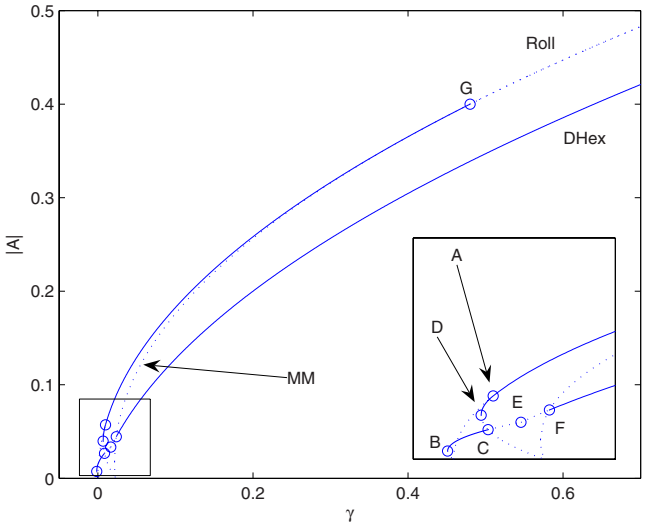

FIG. 4. (Color online) Bifurcation diagram for $p=-1.0$, $\alpha_0=0.2$. Rolls become unstable at point G. The boxed region is qualitatively similar to Fig. 3.

or mixed-mode patterns are stable. An example is shown in Fig. 3. At point E, which exists for all $p<0$, the functional $\alpha[\phi]$ switches sign, and the up hexagons (UHex) become down hexagons (DHex). Down hexagons become stable at point F, after which, there is an infinite bistability region between rolls and hexagons.

For $p<-3/4$, the unstable mixed-mode branch intersects the roll solution and terminates its stability at point G as seen in Fig. 4. Once $\gamma > G$, down hexagons are the only stable pattern.

For $p<-5/4$, there is a sign change in the down-hexagon branch, and the solution cannot exist past a critical value of γ. The stability of this branch is hence terminated at this value of γ via saddle-node bifurcation. This is shown in Fig. 5 by point H. Thus, in this case, there is a region of bistability between down hexagons and rolls between points F and H. After point H, a transition from down hexagons to rolls

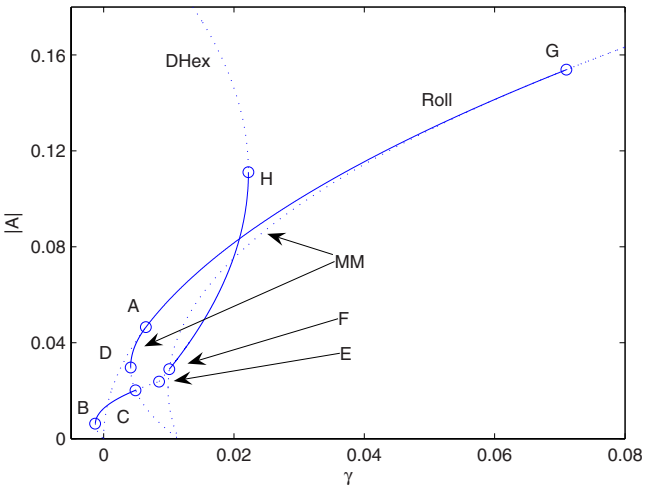

FIG. 5. (Color online) Bifurcation diagram for $p=-1.4$, $\alpha_0=0.2$. Down hexagons become unstable at point H.

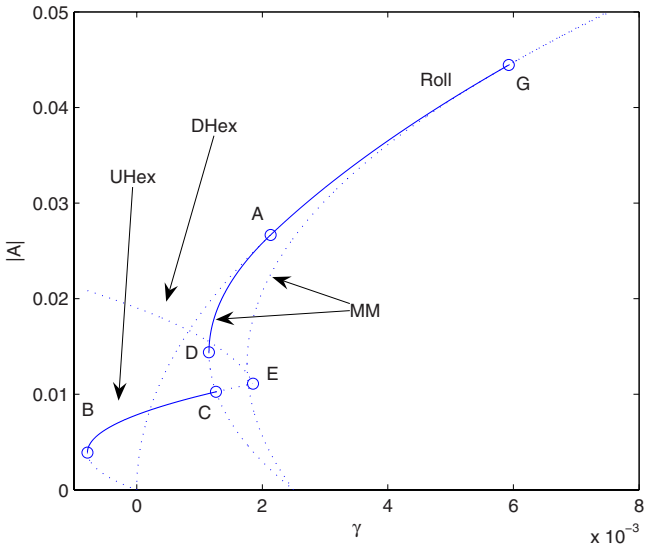

FIG. 6. (Color online) Bifurcation diagram for $p=-3.0$, $\alpha_0=0.2$. Down hexagons are unstable here for all γ.

occurs, and rolls remain stable until point G. After point G, no stable solution of Eqs. (4a) and (4b) exists, and the solution blows up in finite time.

At $p=-9/4$, points F and H from Fig. 5 collide, and down hexagons become completely unstable for any larger values of $|p|$ (see Fig. 6). In this case, with the increase of γ, one observes a transition from up hexagons to the mixed mode at point C. The latter is transformed to rolls at point A.

We solved Eqs. (4a) and (4b) numerically for $\alpha_0=0.2$, $p=-1$, and a range of γ to demonstrate the possibility of stable up-hexagon, roll, and down-hexagon patterns for $p<-1/4$ (bifurcation diagram seen in Fig. 4). A pseudospectral code was used with periodic boundary conditions on a 256×256 grid. The results of these numerical simulations can be seen in Fig. 7. In order to demonstrate stabilization of the mixed-mode (skewed hexagonal) pattern, we solved Eqs. (4a) and (4b) numerically for $\alpha_0=0.2$, $p=-2.5$, and a range of γ corresponding to various values of the ratio m. The results of the numerical simulations are shown in Fig. 8, where one can see the stable skewed hexagonal patterns together with their Fourier spectra. One can clearly see that the amplitude of one mode is larger than that of the two other modes. The amplitude ratio is in excellent agreement with our analytical predictions.

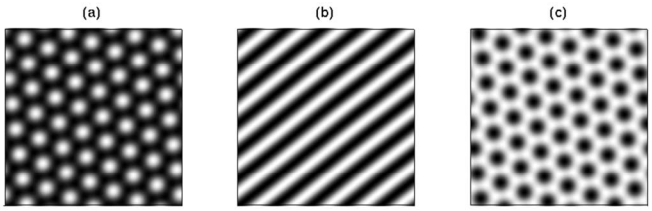

FIG. 7. Numerical simulations of Eqs. (4a) and (4b) showing the possibility of up hexagons, rolls, and down hexagons for $\alpha_0=0.2$, $p=-1$, and $\gamma=$ (a) 0.005, (b) 0.02, (c) 0.04.

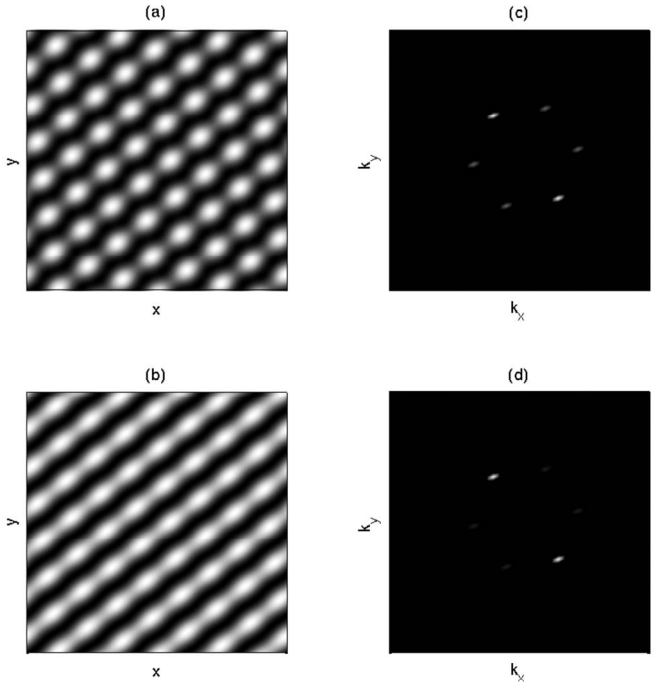

FIG. 8. Numerical simulations of Eqs. (4a) and (4b) showing stable mixed-mode patterns (a),(b) with their corresponding Fourier spectra (c),(d) for $\alpha_0=0.2$ and $p=-2.5$. (a) and (c) correspond to $\gamma=0.001\,59$ $(m=1/2)$, while (b) and (d) correspond to $\gamma=0.001\,95$ $(m=1/6)$.

III. FEEDBACK CONTROL OF SUBCRITICAL DYNAMICS

In this section, we investigate the possibility of using feedback control to suppress the blowup in a subcritical SH equation. We thus consider the following model without delay ($\tau=0$):

$$\frac{\partial\phi}{\partial t}=\gamma[\phi]\phi-(1+\nabla^2)^2\phi+\alpha\phi^2+\phi^3, \tag{13a}$$

$$\gamma[\phi]=\gamma_0-p\max_x\{|\phi|\},\quad (p>0). \tag{13b}$$

In the absence of feedback ($p=0$), the solutions of (13a) and (13b) blow up in a finite time, which means that the model (13a) and (13b) cannot describe the system dynamics. However, as we show below, it is possible to suppress the blowup in the model (13a) and (13b) by means of the chosen feedback control.

A. One-dimensional case

First consider the model (13a) and (13b) in one spatial dimension. Introduce a small parameter $0<\epsilon\ll1$ and consider a weakly nonlinear regime with $\gamma_0=O(\epsilon^2)$. Introduce a long-scale coordinate $X=\epsilon x$ and slow time $T=\epsilon^2 t$, assume $p,\alpha=O(\epsilon)$, and consider the expansion $\phi=\epsilon\phi_1(x,X,T)+\epsilon^2\phi_2(x,X,T)+\epsilon^3\phi_3(x,X,T)+\cdots$, where $\phi_1(x,X,T)=A(X,T)e^{ix}+A^*(X,T)e^{-ix}$. Here we take into account spatial modulations, since patterns with a spatially uniform ampli-

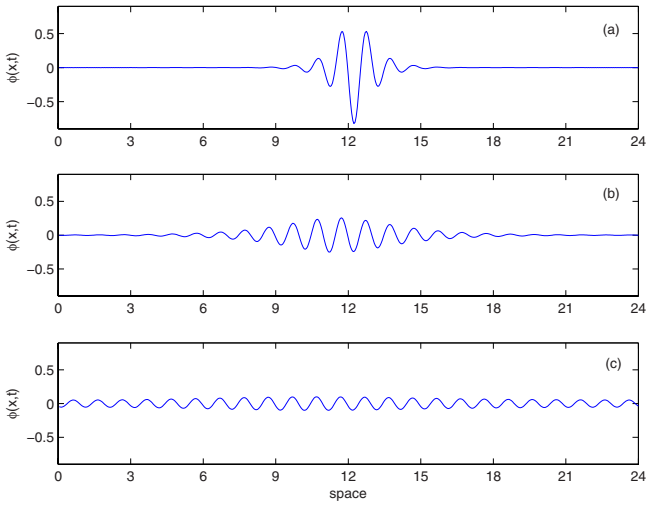

FIG. 9. (Color online) Numerical simulations of Eqs. (13a) and (13b) in 1D for $\gamma_0=1$ and control strengths $p=$ (a) 1.5, (b) 4, and (c) 10.

tude are always unstable. By means of a standard multiple-scale analysis, one obtains, as a solvability condition for ϕ_3 at $O(\epsilon^3)$, the following amplitude equation for the complex amplitude A:

$$\frac{\partial A}{\partial T} = \gamma_0 A - 2p \max_X\{|A|\}A + 3A|A|^2 + 4\frac{\partial^2 A}{\partial X^2}. \qquad (14)$$

Equation (14) is a globally controlled Ginzburg-Landau equation for the complex amplitude of the periodic pattern that occurs near the threshold of linear stability. It was first derived in [32] for the case of global feedback control of morphological instability in directional solidification. As shown in [32], the only stable solution of Eq. (14) is the following localized solution:

$$A(X) = ae^{i\varphi_0}\,\mathrm{sech}[b(X-X_0)], \quad a = \frac{2}{3}p - \frac{2}{3}\sqrt{p^2 - \frac{3}{2}\gamma_0},$$

$$b = \sqrt{\frac{3}{8}}a,$$

where φ_0 and X_0 are arbitrary constants. This solution exists for $p \geq \sqrt{3\gamma_0/2}$ and blows up otherwise. Figure 9 shows stationary numerical solutions of (13a) and (13b) obtained by means of our pseudospectral code (with periodic boundary conditions starting from small-amplitude random noise). One can see the formation of localized spatially oscillating structures whose envelope in a large domain is well described by the solution (15). An increase of the feedback strength p results in the widening of the localized region until it becomes equal to the computational domain, and the solution becomes a modulated periodic structure. Alternatively, an increase in γ_0 narrows the localization region.

Thus, one can see that, in the 1D case, a sufficiently strong feedback control can suppress the blowup in the dynamics described by a subcritical SH equation and lead to the formation of localized patterns.

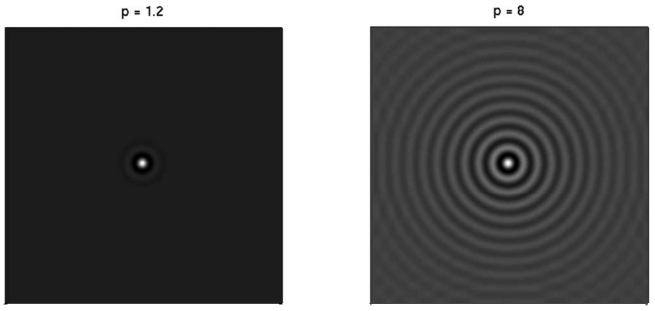

FIG. 10. Numerical simulations of Eqs. (13a) and (13b) in 2D with reflection symmetry ($\alpha=0$). The localized target patterns broaden with increase of the control strength p.

B. Two-dimensional case

Now consider the model (13a) and (13b) in two spatial dimensions. For this case, we have performed numerical simulations of (13a) and (13b) with our pseudospectral code (with periodic boundary conditions and random noise initial conditions) for $\alpha=0$ (systems with reflection symmetry for the order parameter) and $\alpha \neq 0$ (no reflection symmetry for the order parameter). The results are shown in Figs. 10 and 11. One can see the formation of spatially localized patterns. In the absence of a quadratic nonlinearity ($\alpha=0$), a solitary peak evolves from the initial data (see Fig. 10). The peak height is such that the effective linear growth rate $\gamma=\gamma_0 - p\max_x\{|\phi|\}$, is slightly negative, so that the trivial steady state (peak tails) becomes stable. As a result, a spatially localized, radially symmetric structure forms.

In the presence of the quadratic nonlinearity ($\alpha \neq 0$), a spatially localized hexagonal pattern is formed (see Fig. 11).

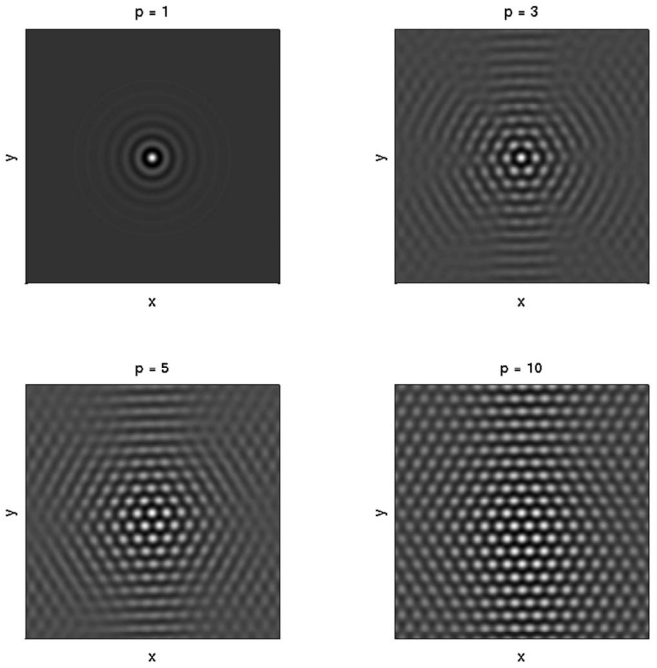

FIG. 11. Numerical simulations of Eqs. (13a) and (13b) in 2D without reflection symmetry ($\alpha \neq 0$). The localized hexagonal structures broaden with increase of the control strength p.

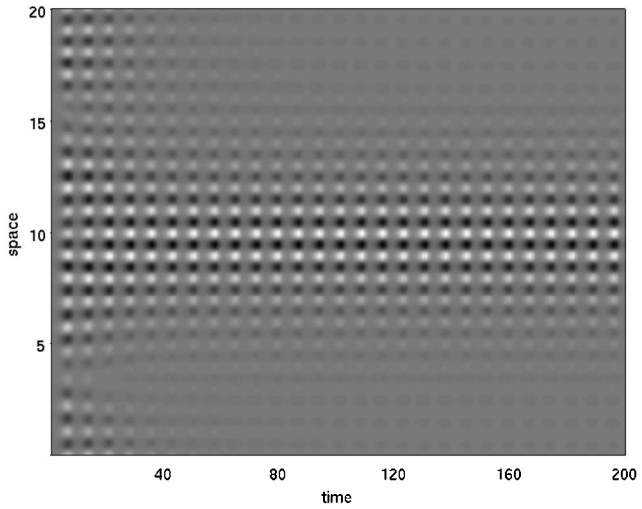

FIG. 12. Spatiotemporal diagram of a numerical solution of Eqs. (13a) and (13b) in 1D with delay for $\gamma_0=1$, $p=4$, $\tau=1.6$, showing a localized structure with oscillating amplitude.

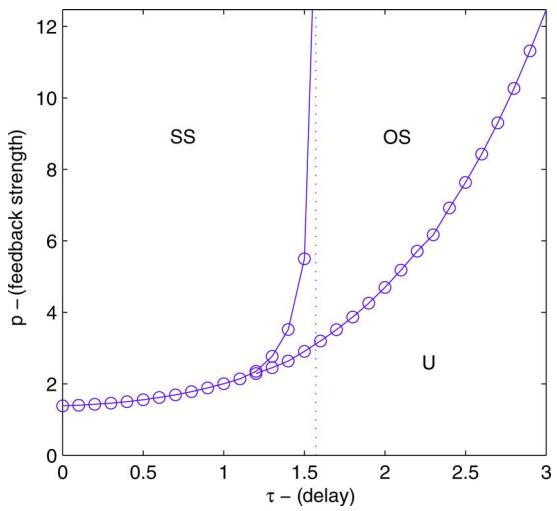

FIG. 13. (Color online) Stability regimes in the (τ,p) plane for Eqs. (13a) and (13b) in 1D at $\gamma_0=1$. SS, stable stationary solutions; OS, stable oscillatory solutions; U, unstable solutions (blowup). The vertical asymptote corresponds to the critical delay value $\tau_c=\pi/2$ for large p.

With increase of the control strength p (or decrease of γ), the localization regions of both types of structure broaden, similarly to the 1D case shown in Fig. 9. The system with $\alpha=0$ approaches a target pattern until it interacts with itself due to the periodic boundary conditions, while the system with $\alpha\neq 0$ approaches a uniform hexagon pattern. Similar localized hexagonal patterns were described in [32].

IV. EFFECT OF DELAY

In this section, we investigate possible effects of feedback delay on the evolution of systems described by (4a), (4b), (13a), and (13b). In the supercritical case with a delayed feedback of the form (2), the delay does not affect the steady-state solutions for small delay values. If the delay is sufficiently large, the system may stabilize to the expected pattern in the absence of control before the feedback is initiated. Once the feedback is then activated, the pattern may still remain in its previous state.

For a subcritical system described by Eqs. (13a) and (13b) with delayed control (3), we have found that, when the delay parameter τ exceeds a certain threshold, the localized structures described in Sec. III undergo a Hopf bifurcation that results in oscillations of the pattern amplitude. A spatiotemporal diagram of this oscillating structure in 1D is shown in Fig. 12.

As the delay is increased, the oscillating amplitude along with the period of oscillation grows. When the delay parameter exceeds another threshold value, the oscillations become unstable, and the solution blows up. A diagram showing stability regimes of stationary and oscillatory solutions is shown in Fig. 13. It is consistent with the stability diagram of a Ginzburg-Landau equation with delayed feedback control obtained recently in [60].

One can see that the stability region of stationary localized solutions has a vertical asymptote in the (τ,p) plane, so that no stable stationary solution exists past this critical value of τ. This critical delay can be found analytically. Indeed, for $p\gg 1$, stationary solutions take the form $\phi\sim R(t)\cos(x-x_0)$. The system finds a balance for long times, such that the effective linear growth $\gamma=\gamma_0-p\max_x\{|\phi|\}\approx 0$, so $R(t)\approx\gamma_0/p$. Then to $O(p^{-1})$ the amplitude of this solution evolves as

$$\dot{R}(t)=\gamma_0 R(t)-pR(t)R(t-\tau). \tag{16}$$

Perturbations of the steady state $\tilde{R}=R-\gamma_0/p$ are described by the linearized equation $\dot{\tilde{R}}(t)=-\gamma_0\tilde{R}(t-\tau)$. Letting $\tilde{R}=e^{i\omega t}$ $(\omega\in\mathbb{R})$, for which the Hopf bifurcation occurs, we find $\gamma_0\tau=\pi(-1)^n(n+\frac{1}{2})$. Since $\gamma_0\tau>0$, this equality is first satisfied for $n=0$. Steady-state solutions are hence stable for $\tau<\tau_c=\pi/(2\gamma_0)$.

In the 2D case, a similar behavior is observed, where an increase of delay induces oscillations in the pattern and an eventual destabilization to blowup. In this case, Eq. (16) and Fig. 13 can also be used for the case $\alpha=0$ in the limit of large p. Figure 14 shows the height of the central peak of the localized target pattern for the case $\alpha=0$ as a function of time. One can see that, below a critical delay, the pattern is stationary, while the peak starts oscillating with a constant amplitude when the delay exceeds this critical value. The $\alpha\neq 0$ case exhibits qualitatively similar behavior. When the delay exceeds a second critical value, the solution blows up.

V. CONCLUSIONS

We have investigated the possibility of active, feedback control of pattern-forming systems using the generic, real Swift-Hohenberg equation (1) as a model. We have considered two types of system: with supercritical and subcritical instabilities. We have shown that, using global feedback control based on measurement of the maximum pattern ampli-

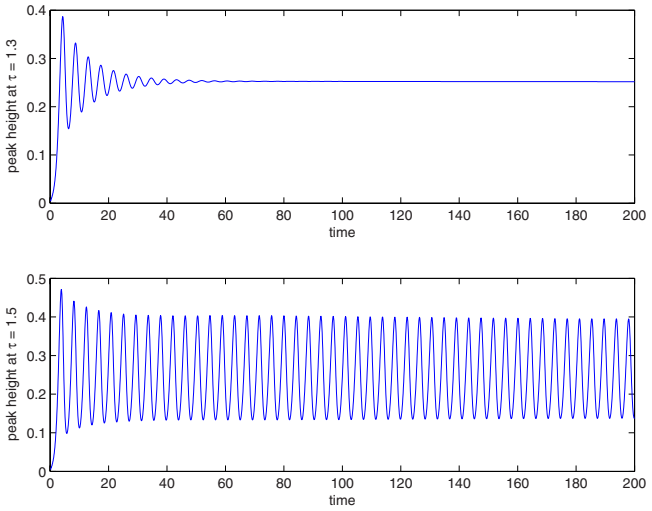

FIG. 14. (Color online) Central peak heights of the target patterns described by Eqs. (13a) and (13b) in 2D as functions of time for $\alpha=0$, $\gamma_0=1$, $p=4$, showing destabilization of stationary structures to oscillatory structures with an increase of delay. τ = (top) 1.3 and (bottom) 1.5.

tude, one can manipulate the competition between patterns with different symmetries (hexagons and rolls) and suppress the blowup in subcritically unstable systems by keeping their dynamics in the weakly nonlinear regime.

For supercritical systems, we have considered feedback control of the quadratic term breaking the reflection symmetry. Within the framework of the model described by Eqs. (4a) and (4b), we have derived a system of amplitude equations with a global control term. The analysis of the solutions of this system shows that the stability regimes of the typical roll and hexagon patterns can be manipulated. The corresponding stability boundaries, given by conditions (6) and (9), are shown to depend on the parameter p, characterizing the control strength. In particular, we have demonstrated that rolls can be completely destabilized for $p \geq 3/4$, and hexagons can be completely stabilized for $1/4 \leq p < 5/4$. For $p < 0$, a transition between up and down hexagons is induced for larger values of γ. In addition, we have shown that, for $p < 0$, feedback control can stabilize the mixed-mode solution corresponding to a skewed hexagonal pattern and found the mixed-mode stability boundaries to be given by (12). Numerical simulations of the system (4a) and (4b) confirm these conclusions. We note that our control method is different from that studied theoretically and experimentally in [29,30], where the Fourier-filtering method was used to control the competition between up and down hexagons, rolls, and patterns with other symmetries in nonlinear optical systems. Instead of applying feedback to the input signal itself, our control method is based on changing physical parameters of the system with feedback from the observed pattern. This could be implemented experimentally by, say, applying an external field to an active medium.

For subcritical systems, we have considered feedback control of the linear growth rate. Within the framework of the model described by Eqs. (13a) and (13b), we have shown that, for sufficient control strengths, the finite-time blowup can be suppressed. We have investigated systems both with and without a reflectional symmetry, corresponding to $\alpha=0$ and $\alpha \neq 0$, respectively. For both types of system, the chosen feedback control leads to the formation of spatially localized structures. In systems with reflection symmetry ($\alpha=0$), the formation of radially symmetric, localized target patterns is observed. In systems without this symmetry ($\alpha \neq 0$), localized hexagonal patterns develop instead. The spatial localization domain increases with increase of the control strength.

We have also investigated the possible effects of delay in the feedback control of Eq. (1). We have found that, in the case of a supercritical instability with feedback control (2), the dynamics remain mostly unchanged for small delay values. For larger delay values, the feedback takes longer to be initiated, and the system has the possibility of stabilizing to the expected pattern in the absence of feedback control. In the case of a subcritical instability with feedback control (3), a sufficiently large delay can induce oscillations of the pattern amplitude. The amplitude of these oscillations grows with an increase of the delay and blows up past a critical delay value. We should note that the feedback delay studied in this paper is different from that used in works such as [61,62], where the delay value was specifically chosen to affect the target pattern. In our analysis, the delay is not chosen at will but is determined from any experimental lag in the feedback loop.

ACKNOWLEDGMENT

This work was supported by the U.S. NSF Grant No. DMS-0505878.

[1] H. Haken, *Advanced Synergetics: Instability Hierarchies of Self-Organizing Systems and Devices* (Springer-Verlag, Berlin, 1983).
[2] A. S. Mikhailov, *Foundations of Synergetics* (Springer-Verlag, Berlin, 1990).
[3] M. C. Cross and P. C. Hohenberg, Rev. Mod. Phys. **65**, 851 (1993).
[4] D. Walgraef, *Spatio-Temporal Pattern Formation: With Examples from Physics, Chemistry, and Materials Science* (Springer-Verlag, Berlin, 1997).
[5] H. G. Schuster, *Handbook of Chaos Control: Foundations and Applications* (Wiley-VCH, Weinheim, 1999).
[6] A. S. Mikhailov and K. Showalter, Phys. Rep. **425**, 79 (2006).
[7] J. Tang and H. H. Bau, Phys. Rev. Lett. **70**, 1795 (1993).
[8] P. K. Yuen and H. H. Bau, J. Fluid Mech. **317**, 91 (1996).
[9] L. E. Howle, Phys. Fluids **9**, 1861 (1997).
[10] J. Tang and H. H. Bau, J. Fluid Mech. **363**, 153 (1998).
[11] H. H. Bau, Int. J. Heat Mass Transfer **42**, 1327 (1999).

[12] A. C. Or, R. E. Kelly, L. Cortelezzi, and J. L. Speyer, J. Fluid Mech. **387**, 321 (1999).
[13] A. C. Or and R. E. Kelly, J. Fluid Mech. **440**, 27 (2001).
[14] P. Kolodner and G. Flätgen, Phys. Rev. E **61**, 2519 (2000).
[15] R. O. Grigoriev, Phys. Fluids **14**, 1895 (2002).
[16] R. O. Grigoriev, Phys. Fluids **15**, 1363 (2003).
[17] P. A. Monkewitz, E. Berger, and M. Schumm, Eur. J. Mech. B/Fluids **10**, 295 (1991).
[18] D. S. Park, D. M. Ladd, and E. W. Hendriks, Phys. Lett. A **182**, 244 (1993).
[19] E. Lauga and T. R. Bewley, Proc. R. Soc. London, Ser. A **459**, 2077 (2003).
[20] E. Lauga and T. R. Bewley, J. Fluid Mech. **512**, 343 (2004).
[21] T. Sakurai, E. Mihaliuk, F. Chirila, and K. Showalter, Science **296**, 2009 (2002).
[22] E. Mihaliuk, T. Sakurai, F. Chirila, and K. Showalter, Phys. Rev. E **65**, 065602(R) (2002).
[23] V. K. Vanag, A. M. Zhabotinsky, and I. R. Epstein, J. Phys. Chem. A **104**, 11566 (2000).
[24] I. R. Epstein, ACS Symp. Ser. **827**, 103 (2002).
[25] D. Lebiedz and U. Brandt-Pollmann, Phys. Rev. Lett. **91**, 208301 (2003).
[26] M. Bertram and A. S. Mikhailov, Phys. Rev. E **63**, 066102 (2001).
[27] M. Bertram and A. S. Mikhailov, Phys. Rev. E **67**, 036207 (2003).
[28] C. Beta, M. Bertram, A. S. Mikhailov, H. H. Rotermund, and G. Ertl, Phys. Rev. E **67**, 046224 (2003).
[29] R. Martin, A. J. Scroggie, G.-L. Oppo, and W. J. Firth, Phys. Rev. Lett. **77**, 4007 (1996).
[30] A. V. Mamaev and M. Saffman, Phys. Rev. Lett. **80**, 3499 (1998).
[31] T. V. Savina, A. A. Nepomnyashchy, S. Brandon, D. R. Lewin, and A. A. Golovin, J. Cryst. Growth **240**, 292 (2002).
[32] A. A. Nepomnyashchy, A. A. Golovin, V. Gubareva, and V. Panfilov, Physica D **199**, 61 (2004).
[33] B. Echebarria and A. Karma, Chaos **12**, 923 (2002).
[34] D. Battogtokh and A. Mikhailov, Physica D **90**, 84 (1996).
[35] D. Battogtokh, A. Preusser, and A. Mikhailov, Physica D **106**, 327 (1997).
[36] Y. Kawamura and Y. Kuramoto, Phys. Rev. E **69**, 016202 (2004).
[37] K. A. Montgomery and M. Silber, Nonlinearity **17**, 2225 (2004).
[38] A. A. Golovin and A. A. Nepomnyashchy, Phys. Rev. E **73**, 046212 (2006).
[39] A. A. Nepomnhyashchy, Physica D **86**, 90 (1995).
[40] G. I. Sivashinsky, Acta Astronaut. **4**, 1177 (1977).
[41] A. Novick-Cohen, Physica D **26**, 403 (1987).
[42] M. L. Frankel, Physica D **27**, 260 (1987).
[43] A. Umantsev and S. H. Davis, Phys. Rev. A **45**, 7195 (1992).
[44] G. M. Homsy, Lect. Appl. Math. **15**, 191 (1974).
[45] A. A. Nepomnyashchy, Fluid Dyn. **9**, 354 (1975).
[46] Y. Kuramoto and T. Tsuzuki, Prog. Theor. Phys. **55**, 536 (1976).
[47] A. Armaou and P. D. Christophides, Physica D **137**, 49 (2000).
[48] T. Kobayashi, Int. J. Syst. Sci. **33**, 175 (2002).
[49] Y. Lou and P. D. Christophides, IEEE Trans. Control Syst. Technol. **11**, 737 (2003).
[50] A. A. Nepomnyashchy and A. A. Golovin, in *Self-Assembly, Pattern Formation and Growth Phenomena in Nano-Systems*, edited by A. A. Golovin and A. A. Nepomnyashchy (Springer-Verlag, Berlin, 2006), pp. 1–54.
[51] J. Swift and P. C. Hohenberg, Phys. Rev. A **15**, 319 (1977).
[52] F. H. Busse, J. Fluid Mech. **30**, 625 (1967).
[53] D. Bensimon, B. I. Shraiman, and V. Croquette, Phys. Rev. A **38**, 5461 (1988).
[54] H. Sakaguchi and H. R. Brand, Physica D **97**, 274 (1996).
[55] A. Handel and R. Grigoriev, Phys. Rev. E **72**, 066208 (2005).
[56] G. H. Gunaratne, Q. Ouyang, and H. L. Swinney, Phys. Rev. E **50**, 2802 (1994).
[57] E. A. Kuznetsov, A. A. Nepomnyashchy, and L. M. Pismen, Phys. Lett. A **205**, 261 (1995).
[58] R. Graham, Phys. Rev. Lett. **76**, 2185 (1996).
[59] A. A. Golovin, A. A. Nepomnyashchy, and L. M. Pismen, J. Fluid Mech. **341**, 317 (1997).
[60] B. Y. Rubinstein, A. A. Nepomnyashchy, and A. A. Golovin, Phys. Rev. E **75**, 046213 (2007).
[61] K. Pyragas, Phys. Lett. A **170**, 421 (1992).
[62] C. M. Postlethwaite and M. Silber, Physica D (to be published).